Available online at www.sciencedirect.com
ScienceDirect
Quaternary Geochronology 1 (2006) 249–260
QUATERNARY GEOCHRONOLOGY
www.elsevier.com/locate/quageo

Research paper

Establishing a chronology for lacustrine sediments using a multiple dating approach—A case study from the Frickenhauser See, central Germany

Dirk Enters[a,*], Gerald Kirchner[b,1], Bernd Zolitschka[a]

[a]*GEOPOLAR, Institut für Geographie, University of Bremen, Celsiusstraße FVG-M, D-28359 Bremen, Germany*
[b]*Institut für Umweltphysik, University of Bremen, D-28359 Bremen, Germany*

Received 17 October 2006; received in revised form 15 January 2007; accepted 18 January 2007
Available online 31 January 2007

Abstract

In order to establish a reliable chronology for lacustrine sediments of the Frickenhauser See (central Germany) different dating methods have been applied. A total of 17 AMS ^{14}C dates, all within the last 2000 years, were supplemented with ^{137}Cs/^{210}Pb dating and varve counting of the uppermost sediments (131 years). The age–depth model for the Frickenhauser See has to cope with highly variable sedimentation rates and overlapping probability distributions of calibrated ^{14}C dates. The uncertainty of calibrated ^{14}C dates could be considerably reduced by including the stratigraphic relationship of the dated samples, the age information derived from short-lived isotopes and varve counting as well as an upper and lower limit of realistic sedimentation rates as 'a priori' information in the calibration procedure. Sets of possible age combinations obtained by repeated sampling from the modified probability distributions were used to calculate continuous age–depth relationships based on monotonic smoothing splines. The obtained age–depth model for the sediment record of the Frickenhauser See represents the average of over 16,000 such model runs and suggests a drastic increase in sedimentation rates from around 1–2 mm a^{-1} (200–1000 AD) to over 25 mm a^{-1} for the period between 1100 and 1300 AD. From then on, sedimentation rates exhibit relatively stable values around 3–9 mm a^{-1}. 'Conventional' age–depth models such as general polynomial regression or cubic splines either do not include the obtained age-information in a satisfying manner (the model being too "stiff") or exhibit "swings" causing age-reversals in the model. Although the age–depth relationships obtained for monotonic smoothing splines and mixed-effect regression are generally very similar, they differ in their respective sedimentation rates as well as in their uncertainties. Mixed-effect regression resulted in much higher sedimentation rates of more than 37 mm a^{-1}. These results suggest that monotonic smoothing splines give better control of the age–depth model characteristics and are well suited in situations, where the integrity of ^{14}C dates is high, i.e. the dated material represents the age of the respective layer.

Keywords: Age–depth modeling; Radiocarbon; Lake sediments; ^{137}Cs; ^{210}Pb

1. Introduction

The significance of paleoenvironmental reconstructions depends on the establishment of independent and reliable absolute chronologies for the studied record (Ojala and Tiljander, 2003). In an effort to identify abrupt climate changes or high-frequency variability, there is an increasing trend to high spatial and temporal resolution of proxy data in paleoclimatic research. Especially in medieval sediments with highly variable detrital input and large uncertainties in ^{14}C dates caused by plateaus in the calibration curve, dating is a major problem in environmental reconstructions (Entwistle et al., 1995). However, only through a precise age control it is possible to compare and correlate results from different sites and/or different types of archives (Bennett, 1994). The success of such attempts is critical to differentiate local effects from regional or even global

*Corresponding author. Present address: UMR CNRS 5204, Environnement Dynamique et Territoires de Montagne Bât. Belledonne, Université de Savoie—Technolac, F-73376 Le Bourget du Lac, France. Tel.: +33 0 4 79 75 87 25; fax: +33 0 4 79 75 87 77.
E-mail address: enters@uni-bremen.de (D. Enters).
[1]Present address: Bundesamt für Strahlenschutz, D-38226 Salzgitter, Germany.

1871-1014/$ - see front matter © 2007 Elsevier Ltd. All rights reserved.
doi:10.1016/j.quageo.2007.01.005

(climatic) signals. Examples include the investigation of synchronicity of events such as the mid-Holocene hemlock (*Tsuga canadensis*) decline in eastern North America (Bennett and Fuller, 2002) or the detection of a synchronous 8200 a cal BP cooling event among several lacustrine sediment archives (Nesje and Dahl, 2001). Dating accuracy is also critical for the determination of synchronicity or possible time lags between cultural developments and shifts in climatic patterns (Berglund, 2003; Tinner et al., 2003). Often, a considerable amount of time and (financial) resources seem to be spent in high-resolution analyses of sediment records whereas less attention is given to the quality of the age control. Thus, unless annual signals provide an internal chronology, there are generally very few age controls in the form of radiometrically dated material, tephra horizons or other stratigraphic markers. Still, "age–depth modeling is perhaps one of the weakest areas in Holocene research and it is an area that urgently requires further attention" (Birks and Heegaard, 2003). Bennett and Fuller (2002) note that "the uncertainty associated with age estimation is greatly enhanced by the uncertainty over which age–depth model to use".

For many lacustrine sediment archives, incremental dating based on varve counting and thus the establishment of an high-resolution chronology is not feasible, since annually laminated sediments are only preserved under special circumstances (Zolitschka, 2003). As a consequence, chronologies often rely solely on ^{14}C dating, which in some cases is supplemented with other information, e.g. tephrochronological data and dating using short-lived isotopes for the uppermost sediment units. ^{14}C dating is the most important dating technique of late Quaternary sediment records, although necessary calibrations to calendar years usually increase the uncertainty associated with each ^{14}C date (Bennett, 1994). The statistical treatment of calibrated dates is complicated by the fact that, unlike the uncalibrated ages, the probability distributions of calibrated ages are not normally distributed and therefore cannot simply be described with common statistical parameters such as mean and standard deviation.

Several publications have provided overviews of various aspects of ^{14}C dating as method, highlighting potential pitfalls and even giving "cook book" style instructions (Oswald et al., 2005; Pilcher, 2003; Björck and Wohlfarth, 2001; Wohlfarth et al., 1998; MacDonald et al., 1991). Nevertheless, there is relatively little information available on which method should be used to construct an age–depth relationship from the obtained dating results (e.g. Heegaard et al., 2005; Birks and Heegaard, 2003; Bennett, 1994). For this reason and because user-friendly programs, which incorporate more sophisticated statistical models, are not available, many age–depth relationships are based on simple linear interpolation, or linear and polynomial regression between point estimates of calibrated ^{14}C dates. There are also several other procedures exist for reconstructing age–depth models, which include Bézier curves (Bennett and Fuller, 2002), fuzzy regression (Boreux et al., 1997) or mixed-effect regression (Heegaard et al., 2005). With exception of the latter (e.g. Dalton et al., 2005), these are rarely applied.

Although Bennett and Fuller (2002) conclude that the commonly used linear interpolation is "rarely unacceptably wrong", serious shortcomings are associated with this method as well as with polynomial regressions:

- A characteristic feature of linear interpolation is a non-continuous first derivative of the age–depth function, i.e. sedimentation rate. In general, abrupt changes of the sedimentation rate occur at each depth, for which an age has been obtained. Consequently, sediment accumulation rates calculated on the basis of sedimentation rates will also show step-like changes, which are not interpretable. If such changes are not accompanied by marked differences in lithology, they are not realistic and represent an inherent problem of linear interpolation.
- For linear interpolation and regression methods, a point estimate of the calibrated probability distribution has to be used. Thus, the information of the full probability distribution is lost. The shortcomings of some of these point estimates are discussed by Telford et al. (2004b). In addition, point estimates of dated objects, which differ in age only by a short period of time, may show apparent age reversals for ^{14}C dates, so that linear interpolation is not applicable.
- The application of simple polynomial functions implies that sedimentation rates are controlled by (simple) physical principles. This may apply in some cases under the assumption of a constant sediment supply, considering for example the effect of sediment compaction or the infilling of an ideal geometric body (such as a lake basin with the shape of an inverted cone). However, sedimentation processes are generally controlled by much more complex factors and thus are unlikely to follow simple models.

In this paper, several dating approaches are used to obtain age information for a lacustrine sediment record of central Germany. The sediment record is characterized by distinct lithological units due to temporary flux of minerogenic matter into the lake caused by anthropogenic soil erosion (Enters et al., 2006). Large variations in sedimentation rates due to erosional input are expected, which must be adequately described by a suitable age–depth model. Therefore, we present a novel procedure to obtain a continuous age–depth relationship based on numerical simulation of calibrated probability density functions of ^{14}C dates (adapted from Bennett 1994) and monotone smoothing splines. Additionally, prior information is used to decrease the date range of ^{14}C dates, such as supplementary age information based on varve counting and short-lived isotopes for the uppermost part of the record, the use of stratigraphical relationships between ^{14}C dates and an upper and lower limit of realistic sedimentation rates between age estimates.

2. Materials and methods

2.1. Site description

The Frickenhauser See is a small, presently meromictic and eutrophic hard-water lake in Lower Franconia, central Germany (10° 14.3′E, 50° 24.1′N, 315 m a.s.l.). The lake was formed by subrosion and has no surface in- or outflow. A steep cliff of Triassic limestone (Unterer Muschelkalk) characterizes the north-eastern side of the lake shore, whereas the more gentle dipping western shore is formed by Triassic sandstone and shales (Oberer Buntsandstein, Rötton). The almost circular lake has a diameter of ca. 110 m and a maximum water depth of 14 m.

2.2. Field work and sediment lithology

In August 2001 and November 2002, sediment cores (FRI A-E) were taken from the central part of the lake with a modified Livingstone piston corer and used to construct a composite sediment profile with a total length of 1275 cm (Fig. 1). In addition, short gravity cores were taken in 2000 (FHS-3, FHS-4) and 2005 (KK1–KK5) to obtain an undisturbed sediment–water interface.

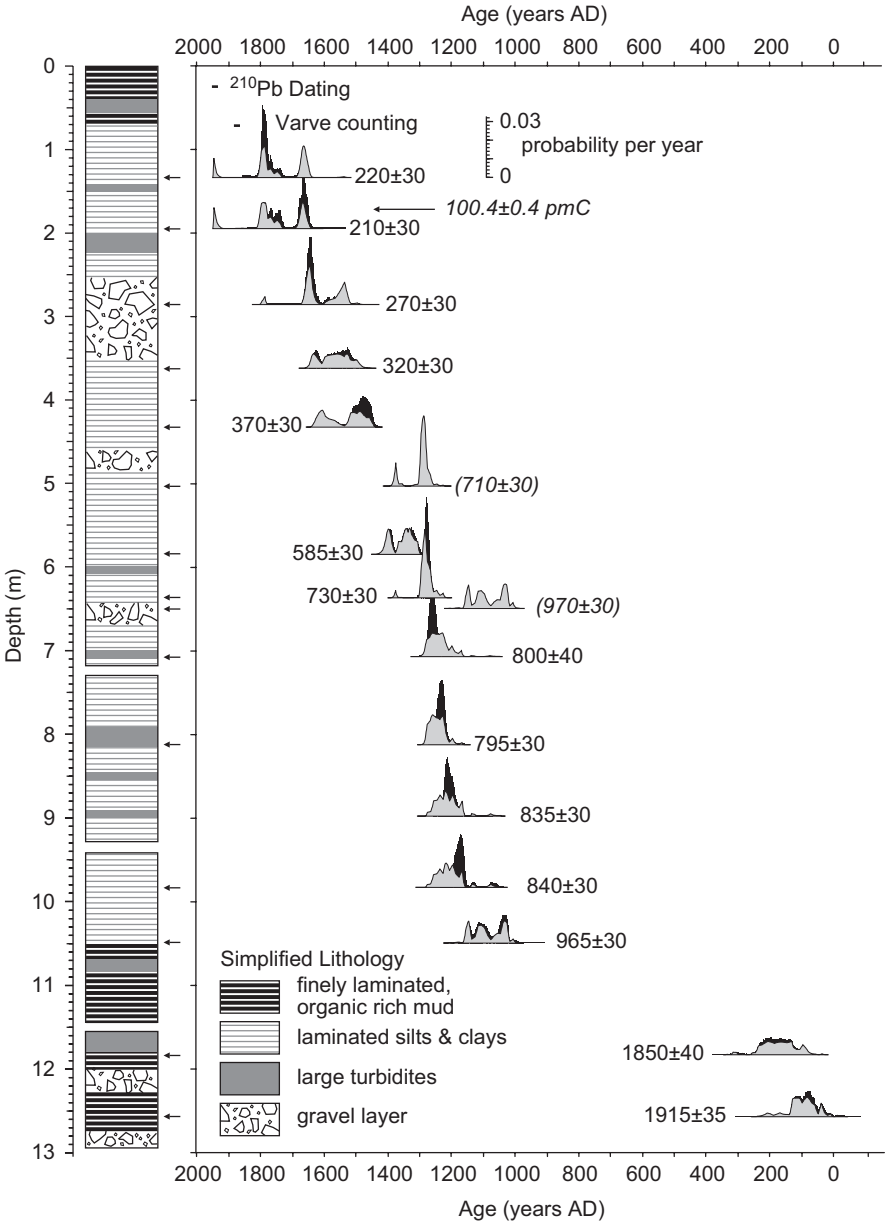

Fig. 1. Stratigraphy and probability density functions (pdf) of AMS ^{14}C dates (described by uncalibrated ^{14}C age and standard deviation) for the Frickenhauser See. Gray pdfs show ^{14}C dates calibrated individually with Oxcal (Bronk Ramsey, 2001), and black pdfs show results obtained by WinBugs calibration using a priori information described in the text. Dates labeled in parentheses were excluded from the reconstruction of the age–depth model. Black arrows on the stratigraphic plot mark the location of the radiocarbon samples.

The lowermost part of the sediment profile (1050–1275 cm, Fig. 1) consists of finely laminated organic-rich gyttja with intercalated layers of fine-grained, small detrital event layers. Sections containing coarse organic detritus and limestone gravel interrupt the laminated sequence. From 73 to 1050 cm depth, the sediment consists of reddish-brown, laminated silts and clays. This facies is characterized by graded layers with highly variable thicknesses of less than 1 mm to more than 10 mm, which are interrupted by thin calcite laminae or black-colored laminae in irregular intervals. Several gravel layers consisting of limestone debris and numerous fine-grained detrital event layers (''turbidites'' of up to 20 cm thickness) occur in this unit. At 73 cm, the lithology changes abruptly to a blackish, sapropelic mud, showing distinct organoclastic lamination with sublaminae of biochemically precipitated calcite.

Up to 718 cm, a composite sediment record was established by visual correlation of overlapping sediment sequences from cores FRI B and FRI D. Only core FRI B reached a final depth of 1237 cm so that three core gaps with an assumed length of 10 cm were included in the profile (Fig. 1). The length of these gaps was estimated by taking the known width of core gaps from the overlapping sequences. Gravel layers and turbidites constitute a significant portion of the total sediment profile (ca. 34%). Since such event layers are deposited almost instantaneously within a short period of time, a modified depth scale (Lanci et al., 2001) was established by excluding event layers that having had thicknesses of more than 2 cm.

2.3. ^{210}Pb and ^{137}Cs dating

The uppermost 29 cm of sediment from core FHS 3 were sampled in continuous 0.5 cm intervals for ^{137}Cs and ^{210}Pb analyses. Determination of activity concentrations of ^{210}Pb and ^{137}Cs was done at the Department of Physics, University of Bremen. Activities of ^{210}Pb (46.5 keV), ^{134}Cs (604 keV), ^{137}Cs (661.6 keV) and ^{214}Pb (352 keV) were obtained γ-spectrometrically using a large-volume reversed electrode high-purity germanium detector (Canberra, 55% relative efficiency). In order to compensate differences in intensity attenuation of low-energy γ-rays of ^{210}Pb due to varying sediment densities, samples were mixed with wax and pressed into pellets of standard geometry and density (Kirchner and Ehlers, 1998). The activity concentration of ^{226}Ra was calculated indirectly from its decay product ^{214}Pb to avoid interferences of ^{235}U with the ^{226}Ra decay line. Unsupported (excess) ^{210}Pb was calculated by subtracting ^{214}Pb activity concentrations measured in equilibrium with ^{226}Ra from the total ^{210}Pb activity concentrations. Age–depth modeling for ^{210}Pb was performed using the constant initial concentration (CIC) model (Appleby, 2001). ^{137}Cs deposition rates were calculated using an advection model fitted to the vertical distribution of ^{137}Cs as described by Kirchner and Ehlers (1998).

2.4. Varve chronology

Thin section analyses were performed on sediment of cores FHS-4 and KK1–KK5. These gravity cores were visually correlated to the composite profile using characteristic marker layers. Preparation of thin sections using freeze-dry techniques followed methods described by Merkt (1971) and Lotter and Lemcke (1999). Laminae were identified microscopically and their thickness measured digitally on images obtained by scanning the thin section on a conventional flatbed scanner equipped with a transparency unit using two polarizing foils.

2.5. ^{14}C dating

In total, 17 samples were submitted to the Poznan Radiocarbon Laboratory, Poland, for AMS ^{14}C age determination. To avoid erroneous ages related to the hardwater effect (Olsson, 1986), all samples submitted for AMS ^{14}C dating consisted of identifiable seeds and leaf fragments of terrestrial plants. In the clastic laminated part of the record, suitable material for AMS ^{14}C dating was generally only found at the basal part of event layers. Where possible, fragile plant fragments (e.g. leaves or complete seed capsules instead of twigs) were submitted assuming that such material would not be preserved during sediment reworking.

2.6. Age–depth modeling

The construction of the age depth model can be divided into two parts: (1) calibrating radiocarbon dates and sampling of the probability density functions of calibrated ages and (2) obtaining a multiple age–depth relationship from sampled ages by monotonic smoothing splines. Apart from the radiocarbon dates, the years 1963 AD at 23 cm and 1870 AD at 51 cm corrected sediment depth with an estimated standard deviation of 3 and 10 years, respectively, were included in the construction of the age–depth model based on the results of the $^{210}Pb/^{137}Cs$ dating and varve counting. In addition, the sediment surface was fixed to 2001 AD (−51 a cal BP).

2.6.1. Calibration and sampling of the probability density functions

Radiocarbon dates were calibrated with WinBUGS (Spiegelhalter et al., 2003) using the 'a priori' information that dates are in stratigraphic order (Buck, 1994) and the requirement of a minimum and maximum time interval between consecutive dates, i.e. an upper and lower limit of the sedimentation rate (0.02 and 5 cm a^{-1}, respectively). The calibration is based on the Intcal04 dataset (Reimer et al., 2004). The initial values for the model were obtained from a normal distribution with a mean equal to the weighted average of the radiocarbon date and a standard deviation of 40 years (Telford et al., 2004a). The model was run using three chains with a burn in of 10,000 iterations

followed by 20,000 iterations, thinned to every 20th iteration. A test for convergence was performed using the potential scale reduction factor (Gelman and Rubin, 1992) implemented in the BOA (Bayesian output analysis) software (Smith, 2005). The output of WinBUGS consists of sets of age estimates for each dated depth, which represent repeated sampling from the modified probability distribution of each radiocarbon date.

2.6.2. Construction of the age–depth model

The set of possible age combinations derived from WinBUGS was used to calculate age–depth relationships by applying monotone smoothing functions adapted from Ramsay and Silverman (2005) using the Matlab® software package. The source code of the smoothing function as well as further details of the method are available under ftp://ego.psych.mcgill.ca/pub/ramsay/FDAfuns/ (last accessed December 2006). This routine uses B-splines of order 6 as basis functions and includes an iterated two-stage minimization of the fitting criterion as penalizing parameter (Ramsay and Silverman, 2002). Sediment depths were treated as independent (predictor) variable and calibrated ages as dependent (response) variable. This procedure yields a smooth, twice-differentiable and strictly monotone age–depth relationship. Thus, the first derivative (i.e. the sedimentation rate) is smooth as well. The applied smoothing function uses knots positioned at each data point (i.e. at each depth of a date) and a smoothing parameter $\lambda = 10^7$. The dates were weighted using the reciprocal of half of the width of 68% calibrated age distribution (i.e. 1/([older border−younger border]/2) Heegaard et al., 2005). Thus, weights are higher if the range of the calibrated age is small.

After the construction of an age–depth model for a selected set of dates the sedimentation rate obtained for each depth was checked against the accepted range. The model was rejected if the minimum or maximum obtained sedimentation rate of the model fell outside the accepted range for sedimentation rates.

2.7. Comparison with other age–depth models

To evaluate the performance of the model, the results are compared with other age–depth relationships. One-sigma ranges and weighted averages of the probability distributions obtained from WinBUGS were used as 68% central calibrated age distribution and point estimates, respectively.

The same set of age combinations as for the monotone smoothing spline was used to calculate an age–depth model based on linear interpolation. A mixed-effect regression model (Heegaard et al., 2005) was calculated using the statistical software package R (http://cran.r-project.org/; last accessed September 2005) and default initial parameters (vspan = 1, $k = n-1$). The simpler model based on constant variance was chosen, as this appeared to give a better fit in the diagnostic plots compared to the μ variance. In addition, age–depth models based on cubic spline interpolation, polynomial regression (order 4–7) and loess smoothing, a curve fitting technique based on local weighted regression, were calculated using the psimpoll software (Bennet, 2005). The root mean square error of prediction (RMSEP) was calculated as a measure of model performance with the smoothing spline age–depth model as reference.

A Poisson-mediated deposition model (p-sequence, Bronk Ramsey, 2007) incorporated in the software OxCal 4.0 (2001; Bronk Ramsey 1995) was applied as additional model evaluation. The parameter k, describing the number of postulated events per unit length, was set to 0.1 cm^{-1} as this value gave an appropriate level of rigidity by allowing relatively large variations in deposition increments. The beginning and the end of the minerogenic sediment unit were included as boundary in the model as sharp changes in sedimentation rates can be expected here.

2.8. Validation

The age–depth model was validated by creating a simulated set of ^{14}C dates following procedures outlined by Telford et al. (2004a). ^{14}C dates were obtained by decalibration from the final age–depth model for (a) the same depths where original ^{14}C dates were taken and (b) the same number ($n = 14$) of ^{14}C dates spaced along equal intervals along the sediment profile. The assumed 'true' age for each depth is converted into a ^{14}C date using the INTCAL04 calibration curve (Reimer et al., 2004). To each ^{14}C date, a single value drawn from a normal distribution with a standard deviation of 30 years was added. This addition simulates the uncertainty that the dated material did not originate at the same time as the sediment interval was deposited and represent the between-object error (Heegaard et al., 2005) caused by contamination or reworking. These new ^{14}C dates together with additional age constraints (^{137}Cs and ^{210}Pb dating, varve formation) were then used to construct age–depth models using the methods described above as well as mixed-effect regression. This step was repeated 10 times for (a) and (b).

3. Results

3.1. Dating results and age–depth model

The chronological controls of the sediment record of the Frickenhauser See are $^{137}Cs/^{210}Pb$ dating and varve counting for the youngest sediments and radiocarbon dates below 1 m sediment depth. OSL dating on the fine quartz fraction as well as pollenstratigraphical correlations with other nearby records failed to give reasonable age estimates that could be included in the age–depth model.

A preliminary varve count interpreting all observed calcite sublaminae as precipitated during successive springs did not agree with the results of radiometric dating

methods. Since apparently more than one calcite precipitation event occurs in the Frickenhauser See within a given year, the criteria used to confine an annual layer were refined. Only massive calcite sublaminae with large ($>20\,\mu m$), idiomorphic calcite crystals were interpreted as the initial start of calcite precipitation when the biological productivity increased in spring. Fig. 2 shows the results of varve counting of the annually laminated part of core KK3 together with the results of ^{210}Pb and ^{137}Cs dating of core FHS 3, which was visually correlated using characteristic marker layers on core photographs. A total of 131 annual layers were identified dating back the onset of regular calcite precipitation in the Frickenhauser See to the year 1870 AD. The average varve thickness is ca. 4.2 mm for the upper part (0–20 cm) and corresponds well with the ^{210}Pb and ^{137}Cs dating. The mean sedimentation rate indicated by the applied CIC model to describe ^{210}Pb activities is $4.74 \pm 0.42\,mm\,a^{-1}$ (± 1 SD). ^{137}Cs activities show distinct peaks that were attributed to 1986 and 1963 (the Chernobyl and weapons fallout maxima, respectively), leading to a sedimentation rate of $4.76 \pm 0.12\,mm\,a^{-1}$. Larger layers with a thickness of 2–3 cm (e.g. at 29 and 34 cm depth) denote increased minerogenic input. There is also a massive slump deposit present from 37 to 53 cm depth, which caused erosion of the underlying laminae in some of the short cores analyzed by thin sections. From 55 cm to 71 cm depth, mean varve thickness decreases to 2.5 mm. However, no ^{210}Pb activities were obtained to confirm this part of the chronology.

The results of the 17 AMS ^{14}C dates are listed in Table 1. Three of the 17 submitted samples had to be excluded for construction of the age depth model due to apparent age reversals or contamination resulting in a modern age. Calibration of the remaining ^{14}C dates using a priori information had a considerable effect on the probability density function of several samples (Fig. 1), decreasing their uncertainty significantly. For example, the probability of the first ^{14}C dates from 133 cm uncorrected

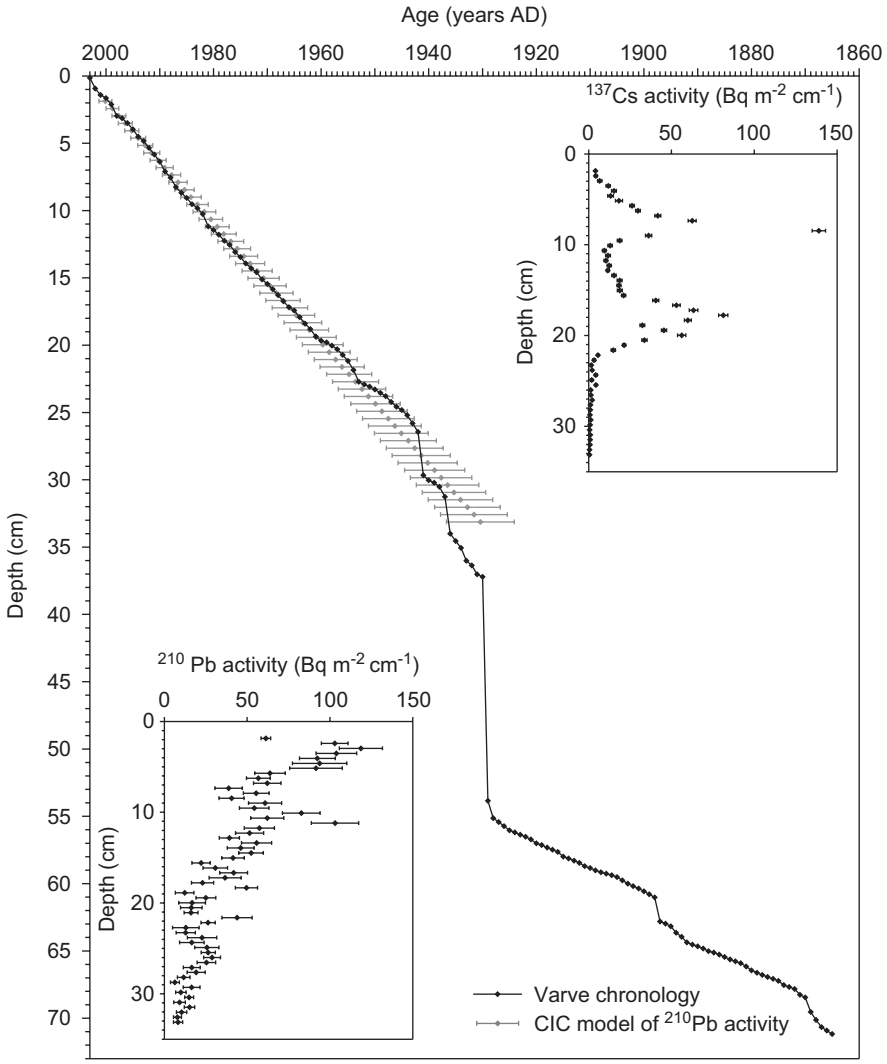

Fig. 2. Age–depth model for the laminated upper part of the sediment sequence of the Frickenhauser See based on varve counts on cores KK2 and KK3 and ^{210}Pb-/^{137}Cs-dating of core FHS3. The ^{210}Pb ages were calculated using a CIC model (Kirchner and Ehlers, 1998), and the error bars indicate the 95% confidence interval. Cores were visually correlated and depths were linearly adjusted to corresponding depths of the composite profile.

Table 1
AMS ^{14}C dates from terrestrial plant macrofossils of Frickenhauser See

	Lab. no.	Sample	Depth (cm)	Corrected depth (cm)	Dated material	$\delta^{13}C$ (‰)	^{14}C Age	Error
1	Poz-8437	B1.2 34–35	133	107	Seeds (*Polygonum arviculare*, *Scleranthus annuus*), seed capsule (*Linum usitatissimum*)	−12.1±0.9	220 BP	30
2	Poz-1550	B2.1 21.5	172.5	137.5	Seeds (*Polygonum arviculare*, *Scleranthus annuus* and others) 100.4±0.4 pmC	−25.1±2.6		
3	Poz-8422	B2.1 43–44	195	155	Seed capsule (*Linum usitatissimum*), seed (*Polygonum arviculare*)	−24.7±0.2	210 BP	30
4	Poz-1557	B2.2 36–38	286	188	Seeds (*Picris hieracioides*, *Linum usitatissimum* and others)	−26.6±1.0	270 BP	30
5	Poz-8423	B3.1 28–29	362	198	Seed capsule (*Linum usitatissimum*), seed (*Hypericum* sp.) and leaf fragments	−27.2±1.0	320 BP	30
6	Poz-1549	B3.1 99–100	433	269	Young twig from *Quercus* sp.	−27.3±1.4	370 BP	30
7	Poz-8439	B3.2 64	502	303	Seed (*Cichorium* sp.), leaf fragments	−27.0±0.2	710 BP	30
8	Poz-8440	B4.1 66.5–67.5	585	361	Seeds (*Polygonum arviculare*, *Scleranthus annuus*)	−21.5±0.3	585 BP	30
9	Poz-8441	B4.2 16–17	636	399	Leaf fragments	−26.9±0.3	730 BP	30
10	Poz-1551	B4.2 30–31	650	402	Seeds (*Scleranthus annuus*), leaf fragments	−26.5±0.8	970 BP	30
11	Poz-8484	B4.2 85–86	706	416	Seeds (*Polygonum arviculare*, *Scleranthus annuus*)	−21.3±2.4	800 BP	40
12	Poz-8442	B5.1 79–83	812	481	Seeds (*Polygonum arviculare*, *Scleranthus annuus*)	−25.7±0.2	795 BP	30
13	Poz-1548	B5.2 70–71	898	531	Seeds (*Polygonum arviculare*, *Scleranthus annuus*, *Chenopodium album*)	−26.7±0.6	835 BP	30
14	Poz-8443	B6.1 42–43	982	609	Seeds (Polygonum arviculare)	−23.6±0.5	840 BP	30
15	Poz-1553	B6.2 12	1049	670	Seed capsule (*Linum usitatissimum*)	−27.1±1.9	965 BP	30
16	Poz-8444	B7.1 29–30.5	1184	781	Leaf fragments	−29.5±3.6	1850 BP	40
17	Poz-1556	B7.2 0.5	1258	829	Leaf fragments (*Populus* sp.)	−31.2±1.0	1915 BP	35

Corrected depth was obtained by subtracting large turbidite deposits (>3 cm), gray-shaded samples are not included in the reconstruction of the age–depth model (see text for further details).

depth (Poz-8437; 220±30 a BP) to be derived from the second half of the 18th century approximately doubles. A narrowing of confidence intervals can also be observed for ^{14}C dates between 6 and 10 m depth (Fig. 1).

The obtained age–depth relationship for the Frickenhauser See is based on a total of 16168 separate model runs and can roughly be divided in three units (Fig. 3). After initial high sedimentation rates of $>1\,cm\,a^{-1}$, sedimentation rates are generally $<0.2\,cm\,a^{-1}$ in the lowest part from 829 to around 680 cm depth (corresponding time period 70–1035 AD). From 680 to 400 cm sediment depth (1035–1280 AD), there is a period of rapid siltation and sediment rates exceed $2\,cm\,a^{-1}$ (maximum sedimentation rate $2.7\,cm\,a^{-1}$). For the remaining part of the record (400 cm to the top), sedimentation rates vary between 0.35 and $0.85\,cm\,a^{-1}$. There is no apparent correlation of the calculated sedimentation rates with other sedimentological proxies such as magnetic susceptibility or dry density (Enters, unpublished data). The period between 1035 and 1280 AD showing the highest sedimentation rates does not reveal noticeable changes in these parameters compared to the rest of the minerogenic sediment unit.

3.2. Comparison with other models and validation

Age–depth models for the Frickenhauser See calculated with different methods show, that both, mixed-effect regression and linear interpolation are relatively similar to the model calculated with monotonic smoothing splines (Fig. 4a–c). This similarity is expressed in a low RMSEP of 28.4 years for mixed-effect regression and 27.3 years for linear interpolation. However, these three models reveal marked differences when respective sedimentation rates and widths of confidence intervals are compared (Fig. 5). Overall, there is a good agreement between sedimentation rates obtained for monotonic smoothing splines and linear interpolation (Fig. 5a). However, the mixed-effect regression model and linear interpolation are characterized by two peaks in sedimentation rates at 460 cm and 580 cm depth, with sedimentation rates exceeding $3.7\,cm\,a^{-1}$ at 460 cm depth in the case of mixed-effect regression. The widths of the 95% confidence intervals reveal additional features of the age–depth models (Fig. 5b). A maximum width of the smoothing spline method is present in the depth interval between 700 and 800 cm, where no ^{14}C date is available and a large change in sedimentation rates

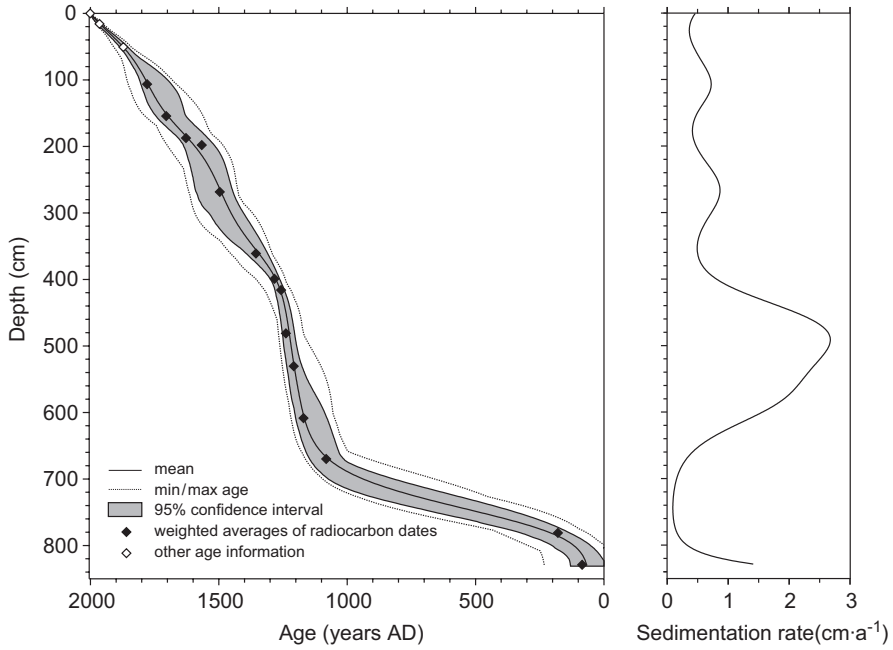

Fig. 3. Age–depth model for the Frickenhauser See and corresponding sedimentation rate calculated using monotonic smoothing splines.

occurs. In contrast, the width of the confidence intervals for mixed-effect regression changes linearly between dates and the values are strongly related to the one-sigma uncertainty of the input data. A characteristic feature of the linear interpolation procedure is that the widths of the confidence intervals generally decrease between ^{14}C dates (Fig. 5b). Minimum widths of the 95% confidence intervals for all age–depth models occur at 400 cm depth, which is caused by two very exceptionally precise ^{14}C dates (Poz-8441, Poz-8484; Table 1) due to a steep calibration curve and by calibration using stratigraphical information.

The Oxcal deposition model conforms well with the monotonic smoothing spline results (Fig. 4a,d). However, the model is too stiff between 560 and 680 cm corrected depth, resulting in slighty older confidence intervals compared with the monotonic smoothing splines and a poor model agreement for radiocarbon sample Poz-8443 at 609 cm depth ($A = 21.5\%$). Because of this, the overall agreement index is relatively low with a value of 68%. Larger values for k, the number of postulated events per unit length, resulted in low overall model agreement indices ($<36\%$). With lower values for k, the model approaches a normal 'sequence', where only the order of radiocarbon dates is taken into account but not sediment depth.

Least-squares line fitting and loess smoothing are "too stiff" and do not fit the data very well (RMSEP = 50.5 years and 67.1 years, respectively). Polynomials with a higher order fit the data well, but show reversals similar to the cubic spline model (RMSEP = 32.0 years; Fig. 4e,f).

For the mixed-effect model, the rejected ^{14}C dates were not included. This allows a calibration of dates using stratigraphical information and thus narrower confidence intervals. However, Heegaard et al. (2005) favor the inclusion of such dates into the model. Taking the two dates into account which were considered as too old (and thus applying individually calibrated ^{14}C dates into the mixed-effect model) gives an unrealistic age–depth model with a sedimentation rate of up to 37 cm a^{-1} (data not shown).

The differences in age–depth models calculated with simulated ^{14}C dates and the final age–depth model are given in Fig. 6 (validation approach). For the monotonic smoothing spline procedure, the average RMSEP is 23.1 ± 4.9 years ($n = 10, \pm 1$ SD) for validation models using simulated ^{14}C dates from the same depths (Fig. 5a) and 28.5 ± 8.0 years for models based on equally spaced ^{14}C dates, respectively. Mixed-effect regressions using the same simulated ^{14}C dates give higher average RMSEP of 34.0 ± 4.5 years (same depth) and 34.70 ± 11.0 years (equally spaced depth intervals).

4. Discussion

4.1. Dating results and age–depth model

The varve chronology could be validated for the uppermost 25 cm by ^{137}Cs and ^{210}Pb dating. The necessary refinement of the initial varve count demonstrates the need of independent dating methods as control and cross-check. The dates of the uppermost core section (varve chronology and results of short-lived isotope dating) fit reasonably well into the age–depth model of the entire record. However, the age–depth model indicates a higher sedimentation rate (0.35 cm a^{-1}) for the lower part of the sapropelic sediment unit compared to the average varve thickness (0.25 cm). This can be explained by a possible abrupt change in

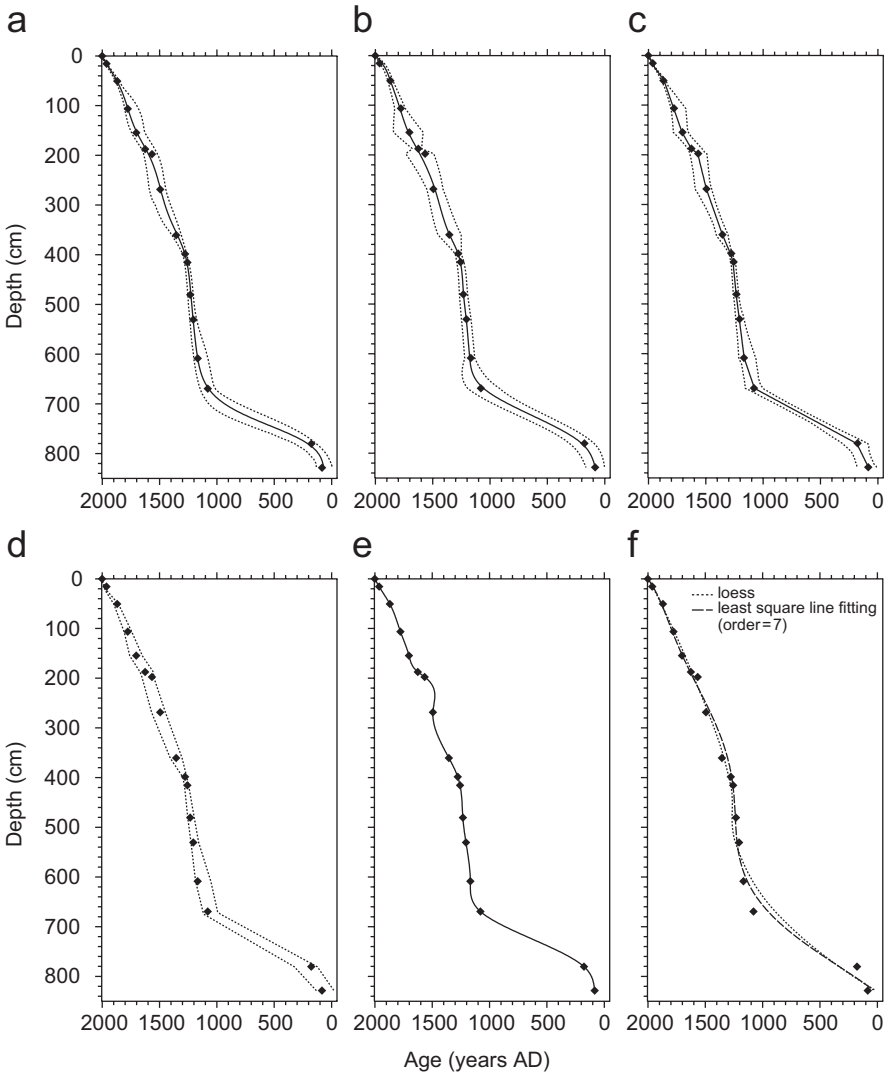

Fig. 4. Comparison of different age–depth models for the Frickenhauser See. The expected age (bold line) and 95% confidence intervals (dashed line) are shown for (a) monotonic smoothing splines, (b) mixed-effect regression, (c) linear interpolation, (d) Oxcal deposition model, (e) cubic spline interpolation and (f) loess smoothing and least-squares line fitting. Black diamonds in each plot mark weighted averages of ^{14}C dates as reference.

sedimentation rates at the onset of organic-rich sediments (i.e. the end of the clastic sediment deposition), which is inadequately described by the age–depth model.

Three out of 17 dates were not included in the age–depth model due to apparent reversals or contamination. However, close inspection of these dates reveals that two of them could fit into the established age–depth model. When sample Poz-1550 (100.4 ± 0.4 pmC) is calibrated using CALIBomb (http://calib.qub.ac.uk/CALIBomb/frameset.html; last accessed December 2006) and the NH_zone1 dataset (Hua and Barbetti, 2004), 8.5% of the area within the two-sigma range accounts for the time interval between 1699 and 1720 AD. This range falls within the 95% confidence interval of the age–depth model for this depth (1642–1772 AD, estimated age 1729 AD). Likewise, sample Poz-8439 at 502 cm uncorrected sediment depth shows a bimodal pdf (Fig. 1). Its younger peak (1350–1390 AD, 14.6% of the two sigma-range) is close to the estimated age for that depth (95% confidence interval: 1399–1533 years, estimated age 1448 AD).

In contrast, sample Poz-1551 appears to be derived truly from reworked sediment as a pollen sample from the same sediment layer does not fit into the general pollen succession (Walter Dörfler, University of Kiel, pers. comm.).

To exclude unrealistic age–depth models, upper and lower limits of a maximum and minimum accepted sedimentation rate were set. Very low sedimentation rates within an age–depth model may indicate a hiatus in the sediment record, whereas apparently high sedimentation rates can be caused by a 'duplication' of the sediment sequence due to slumping. For the sediment record of the Frickenhauser See, however, there is no evidence of a major hiatus in the sediment record. Similarly, no duplicate sections could be detected visually and in various sedimentological parameters.

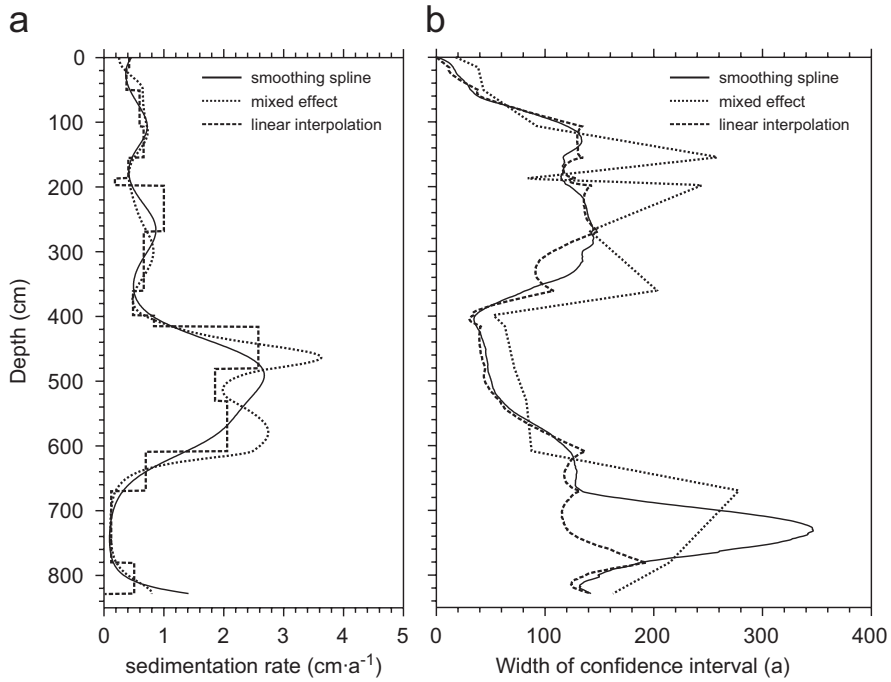

Fig. 5. Comparison of (a) sedimentation rates and (b) widths of confidence intervals for three of the age–depth models shown in Fig. 4.

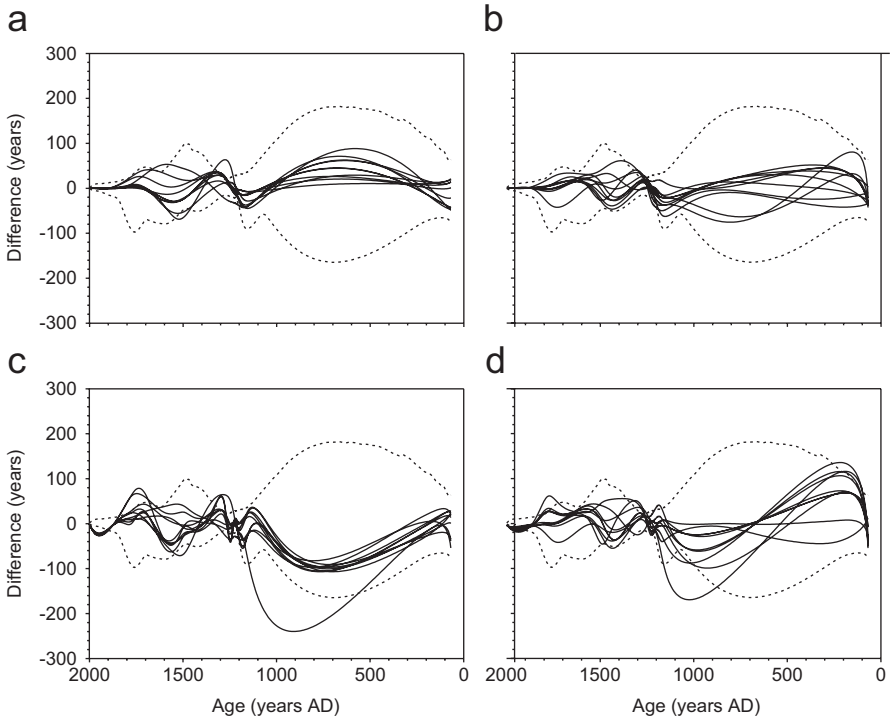

Fig. 6. Plots of the difference between 10 age–depth models calculated by monotonic smoothing splines (a, b) and mixed-effect regression (c, d) using simulated ^{14}C dates at the same depth as the original samples (a, c) and at equally spaced intervals (b, d). Dashed lines are 2.5th and 97.5th percentiles and mark the 95% confidence interval.

The increased sedimentation rates at the bottom of the core have to be carefully evaluated, since these are the effect of only two ^{14}C dates. Higher sedimentation rates might reflect increased soil erosion due to anthropogenic impact prior to the migration period. There is some evidence in the pollen record for agricultural activities in the vicinity of the lake, as the lowermost pollen samples show a marked decrease in arboreal pollen and indicate

more open conditions (data not shown). Another plausible explanation is that this sample was taken shortly after the formation of the lake basin through collapse of the overlying strata. From the initially highly unstable slopes frequent mass movement processes could have caused higher sedimentation rates. If all identified turbidites are excluded, the mean sedimentation rate between the lowermost two ^{14}C dates is on average 0.15 cm a^{-1} (calculated using weighted averages). However, additional ^{14}C dates would be desirable to verify this conclusion.

The essential assumption underlying the procedure proposed here is that the dated material reflects the age of its deposition (i.e. no error in the object to layer relationship), which represents a fundamental difference to mixed-effect regression model of Heegaard et al. (2005). Since the calculated age–depth models are forced to closely follow the distribution of calibrated ^{14}C dates, undetected discrepancies between the age of the dated material and the respective layer will lead to erroneous results. Therefore, dates that do not follow the general stratigraphical sequence have to be excluded prior to age–depth modeling, whereas such dates can be included in the mixed-effect regression model. For the Frickenhauser See, the obtained radiocarbon dates are generally in stratigraphical order, suggesting that the dated objects reasonably reflect the time of deposition.

4.2. Model comparison and validation

The key differences between the results of this procedure and the mixed-effect regression (Heegaard et al., 2005) are (1) the maximum sedimentation rates obtained by each model and (2) the widths of the confidence intervals. Mixed-effect regression shows the highest sedimentation rates in the lower part of the minerogenic sediment unit. Since large turbidite deposits were not included in the depth profile, such values can only be achieved by several small sedimentation/erosion events per year or by duplicate sediment sequences, e.g. caused by a slump. There is, however, no indication of such a feature neither in the lithology of the core nor in any geochemical parameter studied. Monotonic smoothing splines give more realistic sedimentation rates (max. 2.7 cm a^{-1}) considering the setting of the Frickenhauser See with no surface inflow. The uncertainty in the age–depth model calculated by monotonic smoothing splines is highest between radiocarbon dates (700–800 cm depth). Since no age estimate is available, the change in sedimentation rates allows a wide range of possible age–depth relationships. In addition, the widths of confidence intervals are considerably reduced between 100 and 400 cm depth compared to the mixed-effect model. The model validation also shows that monotonic smoothing splines are well suited to model a given age–depth relationship for the Frickenhauser See. The higher RMSEP values in the validation approach for ^{14}C dates taken at equally spaced intervals indicate, however, that both age–depth models are still influenced by the position (depth) of the obtained dates.

5. Conclusion

Absolute chronologies are the prerequisite for the interpretations of sediment records. It is essential to establish reliable age–depth models for such sequences and to evaluate their confidence intervals before comparisons, correlations, and syntheses can be made.

However, the step from discrete age estimates to a continuous age–depth relationship for a paleoenvironmental archive is not a straightforward procedure. ^{14}C dating of sediments younger than a few centuries is problematic because the required calibration gives large confidence intervals due to frequent fluctuations and plateaus of the calibration curve (Björck and Wohlfarth, 2001). However, the consistent transition between the uppermost sediment unit, which has been dated with short-lived isotopes and varve counting, and the youngest ^{14}C dates shows that the use of stratigraphical information can partly reduce this problem. The results presented here indicate that the procedure of monotonic smoothing splines using the full probability distribution of radiocarbon dates is capable to create a realistic age–depth model for the Frickenhauser See. Although the proposed procedure gives the most realistic age–depth model for the Frickenhauser See, it represents only a best guess of reality.

Acknowledgments

This study benefited from the ESF-HOLIVAR program that provided financial support to attend the HOLIVAR workshop course "Holocene dating, chronologies, and age modelling", 24–27 April 2003, Zeist (The Netherlands). Financial support was also received through Grants DFG ZO 102/3-1 and FNK 08/609/1. We thank Felix Bittmann and Steffen Wolters (NIHK Wilhelmshaven) for the identification of macrofossils, Werner Herzer (University of Bremen) for the gamma-spectrometric measurements as well as Tomasz Goslar (Poznań Radiocarbon Laboratory) and Richard Telford (University of Bergen) for helpful discussion. We are also grateful for the helpful comments of two anonymous reviewers.

Editorial handling by: R. Grün

References

Appleby, P.G., 2001. Chronostratigraphic techniques in recent sediments. In: Smol, J.P., Last, W.M. (Eds.), Tracking Environmental Change Using Lake Sediments: Basin Analysis, Coring, and Chronological Techniques. Kluwer, Dordrecht, pp. 171–203.

Bennet, K.D., 2005. Documentation for psimpoll 4.25 and pscomb 1.03. 〈http://www.kv.geo.uu.se/psimpoll.html〉.

Bennett, K.D., 1994. Confidence intervals for age estimates and deposition times in late-Quaternary sediment sequences. Holocene 4, 337–348.

Bennett, K.D., Fuller, J.L., 2002. Determining the age of the mid-Holocene *Tsuga canadensis* (hemlock) decline, eastern North America. Holocene 12, 421–429.

Berglund, B.E., 2003. Human impact and climate changes—synchronous events and a causal link? Quaternary International 105, 7–12.

Birks, H.J.B., Heegaard, E., 2003. Developments in age–depth modelling of Holocene stratigraphical sequences. PAGES News 11, 7–8.

Björck, S., Wohlfarth, B., 2001. ^{14}C chronostratigraphic techniques in paleolimnology. In: Smol, J.P., Last, W.M. (Eds.), Tracking Environmental Change using Lake Sediments: Basin Analysis, Coring, and Chronological Techniques. Kluwer, Dordrecht, pp. 205–245.

Boreux, J.-J., Pesti, G., Duckstein, L., Nicolas, J., 1997. Age model estimation in paleoclimatic research: fuzzy regression and radiocarbon uncertainties. Palaeogeography, Palaeoclimatology, Palaeoecology 128, 29–37.

Bronk Ramsey, C., 1995. Radiocarbon calibration and analysis of stratigraphy: the Oxcal program. Radiocarbon 37, 425–430.

Bronk Ramsey, C., 2001. Development of the radiocarbon program OxCal. Radiocarbon 43, 355–363.

Bronk Ramsey, C., 2007. Deposition Models for Chronological Records. Quaternary Science Reviews 42, in press.

Buck, C.E., 1994. Making the most of radiocarbon dating: some statistical considerations. Antiquity 68, 252–263.

Dalton, C., Birks, H.J.B., Brooks, S.J., Cameron, N.G., Evershed, R.P., Peglar, S.M., Scott, J.A., Thompson, R., 2005. A multi-proxy study of lake-development in response to catchment changes during the Holocene at Lochnagar, north-east Scotland. Palaeogeography, Palaeoclimatology, Palaeoecology 221, 175–201.

Enters, D., Lücke, A., Zolitschka, B., 2006. Effects of land-use change on deposition and composition of organic matter in Frickenhauser See, northern Bavaria, Germany. Science of the Total Environment 369, 178–187.

Entwistle, J.A., Lamb, H.F., Abrahams, P.W., Dogshon, R.A., 1995. A lake-sediment record of changing land-use intensity on the Isle of Lewis, Scotland. In: Butlin, R.A., Roberts, N. (Eds.), Ecological Relations in Historical Times: Human Impact and Adaptation. Blackwell Publishers Limited, Oxford, pp. 45–67.

Gelman, A., Rubin, D.B., 1992. Inference from iterative simulation using multiple sequences. Statistical Science 7, 457–511.

Heegaard, E., Birks, H.J.B., Telford, R.J., 2005. Relationships between calibrated ages and depth in stratigraphical sequences: an estimation procedure by mixed-effect regression. Holocene 15, 612–618.

Hua, Q., Barbetti, M., 2004. Review of tropospehric bomb ^{14}C data for carbon cycle modelig and age calibration purposes. Radiocarbon 46, 1273–1298.

Kirchner, G., Ehlers, H., 1998. Sediment geochronology in changing coastal environments: potentials and limitations of the ^{137}Cs and ^{210}Pb methods. Journal of Coastal Research 14, 483–492.

Lanci, L., Hirt, A.M., Lotter, A.F., Sturm, M., 2001. A record of Holocene climate in the mineral magnetic record of Alpine lakes: Sägistalsee and Hinterburgsee. Earth and Planetary Science Letters 188, 29–44.

Lotter, A.F., Lemcke, G., 1999. Methods for preparing and couting biochemical varves. Boreas 28, 243–252.

MacDonald, G.M., Beukens, R.P., Kieser, W.E., 1991. Radiocarbon dating of limnic sediments: a comparative analysis and discussion. Ecology 72, 1150–1155.

Merkt, J., 1971. Zuverlässige Auszählungen von Jahresschichten in Seesedimenten mit Hilfe von Groß-Dünnschliffen. Archiv für Hydrobiologie 69, 145–154.

Nesje, A., Dahl, S.O., 2001. The Greenland 8200 cal. yr BP event detected in loss-on-ignition profiles in Norwegian lacustrine sediment sequences. Journal of Quaternary Science 16, 155–166.

Ojala, A.E.K., Tiljander, M., 2003. Testing the fidelity of sediment chronology: comparison of varve and paleomagnetic results from Holocene lake sediments from central Finland. Quaternary Science Reviews 22, 1787–1803.

Olsson, I., 1986. Radiometric dating. In: Berglund, B.E. (Ed.), Handbook of Holocene Palaeoecology and Palaeohydrology. Wiley, Chichester, pp. 273–312.

Oswald, W.W., Anderson, P.M., Brown, T.A., Brubaker, L.B., Hu, F.S., Lozhkin, A.V., Tinner, W., Kaltenrieder, P., 2005. Effects of sample mass and macrofossil type on radiocarbon dating of arctic and boreal lake sediments. Holocene 15, 758–767.

Pilcher, J.R., 2003. Radiocarbon dating and environmental radiocarbon studies. In: MacKay, A., Battarbee, R., Birks, J., Oldfield, F. (Eds.), Global Change in the Holocene. Arnold Publishers, London, pp. 63–74.

Ramsay, J.O., Silverman, B.W., 2002. Applied Functional Data Analysis: Methods and Case Studies. Springer, Berlin, 190pp.

Ramsay, J., Silverman, B., 2005. Functional Data Analysis. Springer, New York, 426pp.

Reimer, P.J., Baillie, M.G.L., Bard, E., Bayliss, A., Beck, J.W., Bertrand, C.J.H., Blackwell, P.G., Buck, C.E., Burr, G.S., Cutler, K.B., Damon, P.E., Edwards, R.L., Fairbanks, R.G., Friedrich, M., Guilderson, T.P., Hogg, A.G., Hughen, K.A., Kromer, B., McCormac, G., Manning, S., Ramsey, C.B., Reimer, R.W., Remmele, S., Southon, J.R., Stuiver, M., Talamo, S., Taylor, F.W., van der Plicht, J., Weyhenmeyer, C.E., 2004. IntCal04 terrestrial radiocarbon age calibration, 0–26 cal kyr BP. Radiocarbon 46, 1029–1058.

Smith, B.J., 2005. Bayesian output analysis program (BOA), version 1.1.5 for R. 〈http://www.public-health.uiowa.edu/boa/〉.

Spiegelhalter, D., Thomas, A., Best, N., Lunn, D., 2003. WinBUGS User Manual, Version 1.4. MRC Biostatistics Unit, Cambridge, 60pp.

Telford, R.J., Heegaard, E., Birks, H.J.B., 2004a. All age–depth models are wrong: but how badly? Quaternary Science Reviews 23, 1–5.

Telford, R.J., Heegaard, E., Birks, H.J.B., 2004b. The intercept is a poor estimate of a calibrated radiocarbon age. Holocene 14, 296–298.

Tinner, W., Lotter, A.F., Ammann, B., Conedera, M., Hubschmid, P., Leeuwen, J.F.N.v., Wehrli, M., 2003. Climatic change and contemporaneous land-use phases north and south of the Alps 2300 BC to 800 AD. Quaternary Science Reviews 22, 1447–1460.

Wohlfarth, B., Skog, G., Possnert, G., Holmquist, B., 1998. Pitfalls in the AMS radiocarbon-dating of terrestrial macrofossils. Journal of Quaternary Science 13, 137–145.

Zolitschka, B., 2003. Dating based on freshwater and marine laminated sediments. In: MacKay, A., Battarbee, R.W., Birks, H.J.B., Oldfield, F. (Eds.), Global Change in the Holocene. Edward Arnold Publishers, London, pp. 92–106.